Source contributions to sulfur and nitrogen deposition – an HTAP II multi-model study on hemispheric transport

Jiani Tan[1], Joshua S. Fu[1], Frank Dentener[2], Jian Sun[1], Louisa Emmons[3], Simone Tilmes[3], Johannes Flemming[4], Toshihiko Takemura[5], Huisheng Bian[6], Qingzhao Zhu[1], Cheng-En Yang[1], Terry Keating[7]

[1] Department of Civil and Environmental Engineering, University of Tennessee, Knoxville, TN, USA
[2] European Commission, Institute for Environment and Sustainability Joint Research Centre, Ispra, Italy
[3] Atmospheric Chemistry Observations and Modeling Laboratory, National Center for Atmospheric Research, Boulder, Colorado, USA
[4] Norwegian Meteorological Institute, Oslo, Norway
[5] Research Institute for Applied Mechanics, Kyushu University, Fukuoka, Japan
[6] National Aeronautics and Space Administration Goddard Space Flight Center, Greenbelt, MD, USA
[7] US Environmental Protection Agency, Washington, DC, USA

Correspondence to: Joshua S. Fu (jsfu@utk.edu)

Abstract. With the rising anthropogenic emissions from human activities, elevated concentrations of air pollutants have been detected in the hemispheric air flows in recent years, aggravating the regional air pollution and deposition issues. However, regional contributions of hemispheric air pollution to deposition at global scale have been given little attention in the literature. In this light, we assess the impact of hemispheric transport on sulfur (S) and nitrogen (N) deposition for 6 world regions: North America (NA), Europe (EU), South Asia (SA), East Asia (EA), Middle East (ME) and Russia (RU) in 2010, by using the multi-model ensemble results from the 2nd phase of Task Force Hemispheric Transport of Air Pollution (HTAP II) with 20% emission perturbation experiments. About 27-58%, 26-46% and 12-23% of local S, NO_x and NH_3 emissions are transported and removed by deposition outside of the source regions annually, with seasonal variation of 5% more in winter and 5% less in summer. The 20% emission reduction in source regions could affect 1-10% of deposition on foreign continental regions and 1-14% on foreign coastal regions and the open ocean. Significant influences are found from NA to the North Atlantic Ocean (2-14%), and from EA to the North Pacific Ocean (4-10%) and western NA (4-6%) with 20% emission reduction in source regions. The impact on deposition caused by short-distance

transport between neighbouring regions (i.e. EU and RU) occurs throughout the whole year (slightly stronger in winter), while the long-range transport (i.e. from EA to NA) mainly takes place in spring and fall, which is consistent with the seasonality found for hemispheric transport of air pollutants. Deposition in emission intensive regions such as EA is dominated (~80%) by own region emission, while deposition in low emission intensity regions such as RU is almost equally affected by foreign emission (40-60%) and own region emission. We also find that deposition on the coastal regions or the near-coastal open ocean is twice more sensitive to hemispheric transport than non-coastal continental regions, especially for regions (i.e. west coast of NA) in the downwind location of emission source regions. This study highlights the significant impact of hemispheric transport on the deposition of coastal regions, the open ocean and low emission intensity regions. Further research is proposed for improving ecosystem and human health, with regards to the enhanced hemispheric transport.

1 Introduction

The increasing consumption of energy by human activities has largely increased the deposition of nitrogen (N) over the terrestrial and marine ecosystem (Kim et al., 2011; Galloway et al., 2008; Duce et al., 2008). The impact is estimated to continue increasing in the near future (Bleeker et al., 2011; Lamarque et al., 2013; Kanakidou et al., 2016; Paulot et al., 2013; Lamarque et al., 2005; Bian et al., 2017). The NO_x emission has increased by about 10 Tg(N) from 2001 to 2010, due to large increase in Asia regions (Tan et al., 2018), but the recent studies report a turning point for Chinese NO_x emission in 2011 (Li et al., 2017; Liu et al., 2016). On the other hand, the global sulfur (S) emission has declined by about 5 Tg(S) from 2000 to 2010 (Tan et al., 2018). The global fossil fuel SO_2 emission has a decreasing trend since 1980 owing to the significant decline in SO_2 emission from Europe (EU) and U.S. (Chin et al., 2014). The SO_2 emission in China experiences increases from 2000-2005 due to energy consumption and decreases after 2006 thanks to the implementation of Flue-Gas Desulphurization system. Deposition supplies the ecosystem with nutrients, but too much deposition could cause various adverse impacts on the environment, including acidification and eutrophication of the forest and waterbody (Bouwman et al., 2002; Bergstrom and Jansson, 2006; Dentener et al., 2006; Phoenix et al., 2006), soil acidification that slows down the crop production (Guo et al., 2010; Janssens et al., 2010) and even destroying the

plant biodiversity (Bobbink et al., 2010; Clark and Tilman, 2008). The prevention and control of exceeding deposition have become a growing worldwide concern.

Hemispheric transport of air pollutants is found to aggravate the regional air pollution issues (Wild and Akimoto, 2001; Sudo and Akimoto, 2007; Fu et al., 2012; Fiore et al., 2009) as well as enlarge the local deposition burden (Glotfelty et al., 2014; Sanderson et al., 2008). The mass of aerosols arriving at the North American coasts is comparable to that emitted domestically (Yu et al., 2012). Air pollution from Asia contributes to the $PM_{2.5}$ concentration in western U.S. by 1.5 μg m^{-3} (Tao et al., 2016), the O_3 concentration by 3-10 ppbv (Zhang et al., 2009; Zhang et al., 2008; Yienger et al., 2000; Reidmiller et al., 2009; Jacob et al., 1999; Brown-Steiner and Hess, 2011) and the peroxyacyl nitrate (PAN) concentration by 26 ppbv (Berntsen et al., 1999) in spring. The long-range transport of air pollution from North America (NA) is estimated to contribute by 3-5 ppb (7-11%) to the O_3 concentration in EU annually (Auvray and Bey, 2005; Guerova et al., 2006; Derwent et al., 2004; Li et al., 2002) and the increment can reach 25-28 ppbv during particular events (Guerova et al., 2006). European outflow affects the surface O_3 concentration in western China by 2-6 ppbv in spring and summer (Li et al., 2014) and North Africa by 5-20 ppbv in summer (Duncan et al., 2008; Duncan and Bey, 2004). The study by Yu et al. (2013) found that the long-range transport contributes by 6-16% and 22-40% to aerosol optional depth and direct radiative forcing in 4 regions including NA, EU, East Asia (EA) and South Asia (SA). Recent studies have reported an increasing trend in the hemispheric transport of air pollution from Asia to NA from mid-1980s to late-2000s. The Asian plume has contributed ~10 ppbv (30%) to the O_3 concentration over western NA from mid-1980s to mid-2000s (Jaffe et al., 2003; Parrish et al., 2004), with an annal increase of 0.34-0.50 ppbv O_3 (Parrish et al., 2009). More recent study showed the contribution is about 5-7 ppbv O_3 in 2006 with an annual increase rate of 1-2 ppb O_3 since 2000 (Zhang et al., 2008). The trend well agreed with the rapid growth of Asian emission (Richter et al., 2005; Lu et al., 2010; Verstraeten et al., 2015; Zhang et al., 2007; van der A et al., 2006; van der A et al., 2008).

Compared to the impact on air pollution, the impact of hemispheric transport on deposition hasn't been fully studied. Arndt and Carmichael (1995) developed a source-receptor (S-R) relationship for S deposition among the Asia regions in early 1990s. Zhang et al. (2012) found that foreign anthropogenic emission contributes to 6% and 8% of the oxidized nitrogen (NO_y) and reduced nitrogen (NH_x) deposition in contiguous U.S., respectively. A systematic study by

Sanderson et al. (2008) shed light on the impact of long-range transport on NO_y deposition at global scale. The study used the model ensemble results from the 1st phase of Task Force Hemispheric Transport of Air Pollution (HTAP I) to calculate the S-R relationship for NO_y deposition in 2001 among 4 regions: EU, NA, SA and EA. Results showed that about 12-24% of the NO_x emission was transported and deposited out of source regions. About 3-10% of the emission was deposited on the other 3 regions and affects their deposition by about 1-3%. However, these studies focused on the emission intensive regions, where the foreign disturbance could be relatively small compared to huge own region emission. The foreign impact on low emission intensity regions was not evaluated in the same detail. Furthermore, both the magnitude and spatial distribution of S and N emission and deposition have been changed considerably during the last 10 years (2001-2010) (Tan et al., 2018). It is necessary to update the S-R relationship for more recent years with regards to these changes.

To explore these questions, this study assesses the impact of hemispheric transport of S, NO_x and NH_3 emissions on S and N deposition, with multi-model ensemble results from the 2nd phase of HTAP (HTAP II). Additional to the 4 regions: NA, EU, SA, EA used in Sanderson's study for HTAP I, we include 2 more regions: Middle East (ME) and Russia, Belarussia, Ukraine (RU) in this study. These two regions have low S and N emissions relative to their areal extent, but are located close to the high emission regions such as EU, SA and EA. We calculate the amount of deposition brought by hemispheric transport by comparing model results between the base case and the 20% emission perturbation cases. The experimental design is described in Section 2. Section 3 is the result part and has 3 subsections. We explore the following questions:

1) What fraction (percentage) of the S or N emissions is transported and deposited outside of each source region? What is the fraction of emission that finally deposited on the other 5 receptor regions and oceans? What is the seasonality of the exported fraction?
2) As receptor regions, how much deposition is brought by hemispheric transport? What is the impact on local deposition? Is there any seasonality for this impact?
3) For each region, what are the contributions on deposition of hemispheric transport from foreign regions and of own region emission? In line with the analysis for other pollutants, to this purpose we evaluate the so-called response to extra-regional emission reduction (RERER) metric. We also discuss the own region and foreign impact on the coastal regions specifically. The inter-model variations are also illustrated.

Section 4 is a summary of the findings in this study and some suggestions for future study.

2 Methodology

2.1 HTAP II and experiment set-up

The HTAP was created in 2004 under the Convention on Long-range Transboundary Air Pollution (CLRTAP). It involves efforts from international scientists aiming at understanding the hemispheric transport of air pollutants and its impact on regional and global air quality, public health and near-term climate change. Until now, two phases of HTAP experiments have been conducted successfully. The HTAP I involved more than 20 models from international modeling groups, with 2001 as the base year for modeling studies. A comprehensive report of the major findings of HTAP I was released in 2010 and could be downloaded from http://www.htap.org/. The HTPA II was launched in 2012, with 2010 as the base simulation year. HTAP II required all models to use the same prescribed anthropogenic emission instead of using the best estimates of emission by each modeling group as HTAP I. This facilitates an inter-model comparison between models. In addition, HTAP II had a refined definition for the boundaries of regions, which enabled an update in the S-R relationships for air pollutants and deposition among regions.

This study uses the ensemble of 11 global models from HTAP II (including CAM-Chem, CHASER_re1, CHASER_t106, EMEP_rv48, GEMMACH, GEOS5, GEOSCHEMAJOINT, OsloCTM3v.2, GOCARTv5, SPRINTARS and C-IFS_v2). A detailed description of the experiment set-up could be found in Galmarini et al. (2017). The S deposition includes SO_2 deposition and SO_4^{2-} deposition. N deposition is categorized to NO_y and NH_x deposition. NO_y deposition is a sum of all oxidized N except N_2O, including NO_2, HNO_3, NO_3^-, PAN and other organic nitrates than PAN (Orgn). NH_x deposition includes NH_3 deposition and NH_4^+ deposition. To form the multi-model ensemble, we re-grid all models to a uniformed horizontal resolution of $0.1° \times 0.1°$. We use the multi-model mean value (MMM) of all models to present the ensemble results, a procedure which has been proven previously to have a better agreement with observations than single model result (Dentener et al., 2006; Tan et al., 2018). The multi-model mean values of the compositions of S or N deposition are calculated separately and then combined to compute the total S or N deposition. More details can be found in Tan et al. (2018).

2.2 Simulation scenarios

The base simulation uses anthropogenic emissions in 2010 (Janssens-Maenhout et al., 2015), which is called "base case" in this study. The MMM performance on wet deposition has been evaluated with observations from National Atmospheric Deposition Program (NADP) (http://nadp.sws.uiuc.edu/, last access: 6 April 2018) for NA, European Monitoring and Evaluation Programme (EMEP) CCC reports (http://www.nilu.no/projects/ccc/reports.html, last access: 6 April 2018) for EU and Acid Deposition Monitoring Network in East Asia (EANET) (http://www.eanet.asia/, last access: 6 April 2018) for EA in the previous study of Tan et al. (2018). Following are some brief results of the evaluation results. Modeled gas phase SO_2 wet deposition and aerosol SO_4^{2-} wet deposition are evaluated with observed SO_4^{2-} wet deposition. 76% of the stations of all networks are predicted within ±50% of observation. Negative model biases (-20%) are found at some East Asian stations. Modeled gas phase HNO_3 wet deposition and aerosol NO_3^- wet deposition are compared with observed NO_3^- wet deposition. 83% of the stations of all networks are within ±50% of observation. The European and Southeast Asian stations with high observed NO_3^- wet deposition are somewhat underestimated. Modeled gas phase NH_3 wet deposition and aerosol NH_4^+ wet deposition are compared with observed NH_4^+ deposition. 81% of modeled NH_4^+ wet deposition at stations of all networks are within ±50% of observation. A general underestimation is found in modeled NH_4^+ wet deposition, especially at East Asian stations. In terms of dry deposition, due to the lack of directly measured data, we compare the modeled dry deposition with inferential data from the Clean Air Status and Trends Network (CASTNET) over U.S. The CASTNET data is calculated with observed aerosol concentration and modeled dry deposition velocity, therefore it might have high uncertainty in data quality. Comparison shows that the modeled dry deposition is generally higher than the CASTNET inferential data by a factor of 1-2. This is a common feature of many global and regional models (WMO, 2017). According to the analysis, the model bias for dry deposition mainly comes from the model over-prediction of air pollutant concentration. The CASTNET sites are generally located in remote regions with relatively lower air pollutant concentrations than urban regions, but the models fail to represent this characteristic with coarse spatial resolution (Tan et al., 2018).

HTAP II defines the boundaries of 17 regions as shown in Fig. 1. The emission perturbation experiments are conducted separately for 6 regions (regions with color in Fig.1) with high priority: NA, EU, SA, EA, ME and RU. In the perturbation experiments, the anthropogenic emissions

(including NO_X, SO_2, NH_3, VOC, CO and PM) of a specific region are reduced by 20% from the amounts in the base case simulation, while the emissions in other regions keep constant. In addition, a global perturbation experiment referred as "GLO" is conducted with 20% reduction of global anthropogenic emissions. We estimate the impact of hemispheric transport on deposition by comparing the model results under perturbation experiments with those under base case simulation. In order to validate the quality of model outputs, we check the mass balance between emission and deposition at global scale. The mass balance check for base case simulation is shown in Tan et al. (2018), therefore we show the mass balance for perturbation experiments in this study. We compare the global total amounts of changes of deposition (Δ Depo) with changes of emissions (Δ Emis) for all perturbation cases (Table S1). Models are excluded if their global Δ Depo values fall outside the range of ±20% of their global Δ Emis. According to our results, the amounts of Δ Depo are almost equivalent to Δ Emis for all perturbation cases except the NH_x deposition under EA case. The Δ Depo of NH_x deposition under EA case is not available due to lack of model results for the NH_4^+ wet deposition under 20% emission perturbation in EA.

3 Results

3.1 Export of S and N emissions from source regions

This section studies the export of S and N emissions and oxidation products from source regions. Table 1 shows the S-R relationship of S and N deposition among the 6 regions. The numbers are the sensitivity ($SEN_{r\rightarrow s}$) of deposition in the receptor/source regions to emission changes in the source regions (Sanderson et al., 2008). The metric is calculated as Δ Depo in the receptor/source regions divided by Δ Emis in the source regions following Eq. (1).

$$SEN_{r\rightarrow s} = \frac{\Delta\, Depo\ (r/s)}{\Delta\, Emis\ (s)} \times 100\% \qquad (1)$$

where s is the source region and r is the receptor region. Δ Depo (r/s) is the deposition change in the receptor/source regions, Δ Emis (S) is the emission change in the source regions. This value indicates the fraction of emission of source regions that is deposited locally or exported to foreign regions.

The numbers outside of the parenthesis in Table 1 are for coastal and non-coastal regions together and the numbers in the parenthesis are specifically for coastal regions (defined in Fig. 1).

"Others" means the other regions in the world than the 6 regions (white color in Fig.1). The NA region has 69% of its S emission deposited within itself, including 9% deposited on its coastal region. The remaining 31% is exported to the other regions, mostly to the "Others" and less than 3% is deposited on the other 5 regions (EU, SA, EA, ME and RU). A relatively large fraction (14 %) of European S emissions are exported to RU region. Other major pathways of export of S emissions/reaction products are from SA to EA (9%), from EA to RU (5%) and from RU to EU (7%) and EA (5%). ME has considerable percentages of S emission exported to its nearby regions such as SA (8%), EA (5%) and RU (5%). The S-R relationship of NO_y deposition is similar to that of S deposition, except that EU and ME have 66% and 54% of NO_x emissions deposited within the source region, which are 6% and 12% higher than those of S emissions, likely due to somewhat longer lifetimes of S emission compared to NO_x emission and the large average emission altitude of S emissions. In terms of NH_x deposition, about 20% more NH_3 emission is deposited within the source regions (except ME) compared with S and NO_x emission, due to its short lifetime in the atmosphere.

The seasonal variations of the export of S and N emissions by source regions is shown in Fig. S1. In terms of S emission, there is 5-10% of seasonal differences around the annual average export fractions for all regions except SA. SA exports almost half of its S emission in spring, which is twice the numbers in summer (20%) and fall (25%), related to the specific dry period and monsoon circulation. The seasonal export fractions of NO_x and NH_3 emission are similar to that of S emission in the pattern, but generally lower in values in all seasons. Generally, the source regions export the highest percentage of their emissions in winter and spring and lowest in summer. More proficient oxidation chemistry in summer results in more soluble component, and local weather systems, especially the episodic of precipitation has large influence on this seasonality. For most continental regions, the wet deposition accounts for 50-70% of total deposition (Tan et al., 2018; Vet et al., 2014; Dentener et al., 2006). Therefore, local precipitation plays an important role in the local pollution removal process. On the other hand, for regions with low local precipitation like ME, the percentage of emission removed within own region would be lower than the other regions. In addition, the strong westerly winds in winter and spring favor the hemispheric transport for regions in mid-latitudes of the North Hemisphere. While the rapid vertical convection in summer slows down the zonal transport of air flows and accelerates the local removal process.

A comparison is conducted with previous studies. Bey et al. (2001) estimated that 70% of emitted NO_x from Asia is lost within its boundary by deposition of HNO_3 in spring. The estimation in our study is 70% for EA and 61% for SA, close to Bey's result. Li et al. (2004) reported that about 20% of anthropogenic NO_x emitted by NA is deposited out of its boundary (about 1000 km offshore). Stohl et al. (2002) calculated that 9-22% of surface NO_x emissions is exported out of the boundary layer of NA. Our estimation is about 30%, higher than Li's and Stohl's results. HTAP I study by Sanderson et al. (2008) developed a SR relationship for NO_y deposition among NA, EU, SA and EA. Their results showed that about 12-24% of the emitted NO_x is deposited out of source regions. This study of HTAP II finds a higher percentage of export (26-34%). It should be noted that the estimations of different studies are influenced by several factors and the results are not fully comparable: (1) Definition of boundaries of source and receptor regions. For instance, Li et al. (2004) defined the boundary of NA by a squared domain: 65-130°W, 25-55°N, while we use the continental boundaries defined by HTAP II. There are also changes in the definition of boundaries from HTAP I to HTAP II. For instance, HTAP I includes Mexico and Central America in NA, but they are defined as a separate region in HTAP II (region 12 in Fig. 1). The boundary of EU is also changed in HTAP II. (2) HTAP I simulations only change the NO_x emission, but HTAP II simulations also reduce the other anthropogenic emissions, including SO_2 and PM. The joint control of multiple species may result in more reduction in NO_y deposition and it is hard to estimate this effect in this study.

3.2 Impact of hemispheric transport on deposition

This section investigates the impact of hemispheric transport on deposition in the receptor regions. Figure 2 is annual response of S deposition to 20% emission reduction in source regions calculated as Eq. (2).

$$Response = \frac{\Delta\, Depo\ (perturbation)}{Depo\ (base)} \times 100\% \qquad (2)$$

where Δ Depo (perturbation) is the Δ Depo between perturbation case and base case. Depo (base) is the deposition under base case. The negative values mean that the deposition decreases with reduction in emission. Table S2 summarizes the regional median deposition fluxes under base case and under emission perturbation cases. Fig. 2(a) shows the global response of S deposition to 20% emission reduction in NA. The largest deposition change is found in the source region NA, with a

4-20% decrease in S deposition in the non-coastal region and 14-16% decrease at the east coast. The impact on the North Atlantic Ocean deposition declines gradually from near coastal region (12-14%) to the open ocean (2-12%) and Eurasia (<1%). Fig. 2(b) shows the global response of S deposition to 20% emission reduction in EU. Although the impact on continental non-coastal regions is high (6-18%), the impact on the coastal regions is generally less than 6%, much lower than NA's impact on its east coast (14-16%). The deposition in North Africa, central Asia and western RU is affected by 2-6%. The 20% emission reduction in SA (Fig. 2(c)) shows large influence over its south-west coast and the Arabian Sea (4-12%). The SA's outflow affects the deposition in southeastern ME and eastern Sub Saharan Africa by 1-4% and western EA and Southeast Asia (mainly Bangladesh) by 2-6%. Fig. 2(d) shows the impact on S deposition from 20% emission reduction on deposition in EA. On one hand, the impact is strong on the east coast of China (12-16%) and decreases gradually over the North Pacific Ocean (4-10%). Although the majority of S emission is deposited on the North Pacific Ocean, the influence on western NA can still reach 4-6%. On the other hand, the impact on Southeast Asia and SA is much lower (2-5% and <1%), due to the block of air flows by the Himalaya Mountains (Fig. S4). The 20% emission reduction in ME mainly affects the S deposition in Africa by 2-10% and western EA by 2-4%. Fig. 2(f) shows the S deposition change with 20% emission reduction in RU. The regions of impact are mainly at high latitudes in the North Hemisphere, including northern EU (2-6%) and western Arctic Circle (1-4%). The Russian flow enters the Arctic in the lower troposphere in winter season (Stohl, 2006).

The impact of NO_x emission reduction on NO_y deposition from each source region is shown in Fig 3. The overall impact is qualitatively similar to that of S emission in the spatial pattern, with some differences in the values. For some regions, the impact of hemispheric transport on NO_y deposition is lower than that on S deposition. For instance, SA's impact on eastern Africa is about 1-4% on S deposition, but is <1% on NO_y deposition. ME's impact on the western Africa and Gulf of Guinea is about 2-4% on S deposition, but is <1% on NO_y deposition. These smaller sensitivities reflect differences in lifetimes, and the lower formation of aerosol nitrate under warm conditions in tropical regions. Under the NA perturbation case (Fig. 3(a)), an 8-12% change of NO_y deposition is found on the west coast of California, due to high NO_x emission in California from mobile source, which is not seen in S deposition. The impact of emission reduction in EU and EA on their coastal regions is generally 2-4% higher for NO_y deposition than S deposition

(Fig. 3(b) and (d)). The impact on NH_x deposition is similar to that on NO_y deposition (Fig. S2). It should be noted that this is the result from 20% emission reduction in the source regions, therefore the actual impact (100% emission reduction) could be 5 times higher when assuming a linear relationship between 20% and 100% emission reduction on deposition.

We quantify the amount of deposition carried by hemispheric transport and study its seasonality. Fig. 4 shows the monthly changes of S deposition for 20% emission reductions in source regions. The values are meridional sum with a west-east resolution of 0.1 degree, and display well the locations of the source regions. The negative values indicate the amounts of pollutants transported from source regions to receptor regions. According to Fig 4(a), NA has about (1-10) $\times 10^4$ kg(S) $month^{-1}$ per 0.1° longitude of its S emission transported and deposited over the North Atlantic Ocean (15-75°W) throughout the whole year. We also find about (1-3) $\times 10^4$ kg(S) $month^{-1}$ per 0.1° longitude decrease of S deposition at about 90°E and 120°E in spring and fall, which gives evidence to NA's influence on Eurasia via transatlantic flow, although this amount accounts for less than 1% of local S deposition (white in Eurasia in Fig.2(a)). Fig. 4(b) shows that about (1-3) $\times 10^4$ kg(S) $month^{-1}$ per 0.1° longitude of EU's emission is transported to and deposited at 30-60°E in RU throughout the whole year and at 100-120°E in EA in spring and fall. According to Fig. 4(c), SA exports its S emission to 30-60°E in ME and eastern Africa in early spring and to 90°E-180° in EA and North Pacific Ocean from late spring until fall. In particular, the influence on EA can reach (5-10) $\times 10^4$ kg(S) $month^{-1}$ per 0.1° longitude in mid-spring. According to Fig. 4(d), EA's S emission is widely transported and deposited over the North Pacific Ocean throughout the whole year. The Asian outflow arrives at the west coast of NA (~130°W) in all seasons except summer, but only reaches far in western NA (~90°W) in spring and brings about 1 $\times 10^4$ kg(S) $month^{-1}$ per 0.1° longitude of S deposition. The export to SA in only found during the Asia winter monsoon. The monthly changes of NO_y deposition with perturbation experiments are shown in Fig. 5. Compared to S deposition, the change in NO_y deposition by hemispheric transport is generally smaller. For instance, the NA's impact on Eurasia is (1-3) $\times 10^4$ kg(S) $month^{-1}$ per 0.1° longitude for S deposition, but is less than 0.5 $\times 10^4$ kg(N) $month^{-1}$ per 0.1° longitude for NO_y deposition. The SA's impact on EA (90-120°E) can reach (5-10) $\times 10^4$ kg(S) $month^{-1}$ per 0.1° longitude for S deposition, but the amount is 4 times lower for NO_y deposition. This result is in accordance with the S-R results in section 3.1 that more S emission is transported out of the source regions than N emission, probably due to longer chemical lifetimes and higher

emission altitudes. Patterns similar to NO_y are also found in the monthly changes of NH_x deposition (Fig. S3).

The deposition change via transport between neighboring regions is found throughout the whole year and is slightly stronger in winter, such as between EU and RU (~30°E) (Fig. 4(b) and (f)) and from EA to the North Pacific Ocean (~130°E) (Fig. 4(d)). This is consistent with the seasonality we found for the export of emission by source regions in section 3.1. In addition, most source regions reduce more S and NO_x emissions in winter than the other seasons (Table S3), thus more emissions are exported abroad in winter. On the contrary, the deposition change by transport over long distance mainly occurs in spring and fall, especially for the hemispheric transport from NA to EU, from EU to EA and from EA to NA. The seasonality of long-range transport for NA, EU and EA well fits the characteristic of westerlies, which is the prevailing winds in the mid-latitude of the North Hemisphere. This agrees with the seasonality of the transpacific, transatlantic and trans-Eurasia flows of air pollutants that spring is the most efficient season for long-range transport for mid-latitudes (Holzer et al., 2005;Liu et al., 2005;Liang et al., 2004;Brown-Steiner and Hess, 2011;Li et al., 2014;Auvray and Bey, 2005;Wild et al., 2004;Liu et al., 2003). Although the westerlies is also strong in winter, the pollution in the air flow is low, because the formation of secondary species like PAN is suppressed by slow oxidation in cold environment (Berntsen et al., 1999;Deolal et al., 2013;Moxim et al., 1996), which plays an important role as a reservoir for NO_x in the long-range transport of air plumes (Lin et al., 2010;Hudman et al., 2004).

3.3 Own region and foreign contributions on deposition

This section compares the contributions between hemispheric transport and own region emission control on deposition. A metric called extra-regional emission reduction (RERER) is calculated by dividing the Δ Depo due to foreign emission reduction by Δ Depo due to global (foreign + own region) emission control following Eq. (3).

$$RERER_i = \frac{\Delta\, Depo_i\,(foreign)}{\Delta\, Depo_i\,(global)} \qquad (3)$$

where i is the region of focus. $\Delta\ Depo_i$ (foreign) is the Δ Depo in region i due to 20% foreign emission reduction. It is calculated by subtracting the Δ Depo due to 20% own region emission

control from Δ Depo due to 20% global emission reduction. Δ $Depo_i$ (global) is the Δ Depo in region i due to 20% global emission reduction. This metric indicates the importance of foreign emission on local deposition. A low RERER value (close to 0) indicates a predominance effect of own region emission on local deposition, while high RERER value (close to 1) means strong impact of hemispheric transport on local deposition.

Table 2 shows the RERER values for total (include both non-coastal and coastal regions), non-coastal and coastal regions. For both non-coastal and coastal regions, the own region impact includes control of both its coastal and non-coastal regions, and the foreign impact comes from emission reduction of foreign coastal and non-coastal regions. As we expected, NA (0.07, 0.17, and 0.17), SA (0.04, 0.17, and 0.18) and EA (0.16 and 0.16) regions have relatively low RERER values, due to large local emissions compared to the foreign contributions. EU (0.12, 0.34 and 0.36) and ME (0.32, 0.32 and 0.42) have relatively higher RERER values. RU is the only region with RERER (0.55, 0.59 and 0.61) higher than 0.5, which means its deposition is almost equally sensitive to foreign impact and own region control. The RERER values NO_y deposition are of similar magnitudes to S deposition, while the RERER of NH_x deposition is 0.1 lower, probably due to the lack of data from EA perturbation case, so that the contribution from EA is not considered.

The RERER values of coastal regions are generally 0.1-0.3 higher than those of non-coastal regions. The values for RU's coast are all higher than 0.84. Even regions with low non-coastal RERER such as NA and SA have high RERER on coastal regions. For instance, the RERER of NA reaches 0.3-0.4 for its coastal region, more than double of the RERER on its non-coastal regions (0.05-0.12). Coastal regions receive high proportion of deposition from foreign transport. Except large scale circulation like prevailing westerlies, the coastal regions are featured with complex small scale circulations. For instance, the low-level jet (zonal winds with high speed) contributes to the rainfall in coastal regions in Asia (Xavier et al., 2018). The orographic effects enhance the precipitation over coastal mountain regions such as west coast of NA, EU and southeast coast of RU (James and Houze, 2005). According to table 1, EA exports 5% of its S and N emission to RU, almost half of which is deposited on RU's coastal regions. RU exports 7-12% of S and N emission to EU, of which 30% is deposited on EU's coastal regions. The impact of hemispheric transport is identical or even larger than the effect of own region emission control for

some coastal or near coastal regions. According to Fig. 2, 20% emission reduction in EA can reduce 2-6% of S deposition in the west coast of NA. This effect is even larger than 20% emission reduction in own region emission (<1%). Similarly, 20% emission reduction in NA can change 2-5% of S deposition in west coast of EU, which is almost identical to the effect of 20% emission control in EU. On one hand, the emissions in western NA and western EU are relatively low, thus the effect of own region control is not significant. On the other hand, these coastal regions are in the downwind location of eastern EA and eastern NA, which are the main source regions of S and N emissions. Coastal regions serve as transit places for air-sea exchange with vulnerable ecosystem (Jickells, 2006;Jickells et al., 2017). The over-richness of deposition in coastal water and ecosystem can evoke a number of environmental issues, of which some are specifically for coastal regions such as threats to coastal benthic and planktonic system and sustainability of fishery (Paerl, 2002;Doney et al., 2007).

Figure 6 compares the percentage concentrations on deposition between foreign transport and own region emission. Other (OTH, pattern fill in the figure) is calculated as $\Delta\ Depo_{(GLO)} - \sum \Delta\ Depo_{(case)}$ (case = 6, including NA, EU, SA, EA, ME and RU). It indicates the deposition change due to other reasons than the total effects of separate emission reduction in the 6 regions. It could come from the emission reduction in rest of world, especially nearby regions such as from Central Asia and North Africa to EU and ME. It could also come from the joint effects of emission control by multiple source regions, which possibly change the oxidant chemistry, atmospheric mixing and lifetimes of reactive pollutants. However, the model simulations do not allow to separate these two contributions in this study. For regions with low RERER values (NA, SA and EA), the own region emission dominates the deposition by more than 80%. For these regions, determined by vicinity and transport patterns, the foreign impact is somewhat dominated by certain source regions, such as from EA to NA (2-4% out of 4-5%), from ME to SA (5-6% out of 7-11%) and from SA to EA (3-4% out of 4-7%). For EU and ME, there is about 20% contribution from "OTH". Beside this, RU contributes 4-5% to EU's deposition and EU contributes 5% to ME's deposition. For high RERER regions, RU has a different pattern than the other regions. The contributions of hemispheric transport from the other 5 regions (23-45%) are almost equivalent to its own region emission control (39-45%), with significant contributions from EA (20-24%) and EU (13-15%).

Figure 7 shows the inter-model variation on simulating the Δ Depo of S, NO_y and NH_x under emission perturbation cases, separately for wet and dry deposition. The values are global

integrated changes in component deposition for perturbation experiments from MMM results, with error bars showing the maximum and minimum values of models. The figure only shows main compositions of S and N deposition, which together account for more than 95% of total deposition. In terms of S deposition (Fig. 7(a)), the modeled Δ Depo by multiple models, defined as (maximum value of multi-model – minimum value of multi-model), ranges (0.06-0.23) Tg(N) yr^{-1} and (0.01-0.22) Tg(N) yr^{-1} for SO_2 dry and wet deposition, and (0.01-0.03) Tg(N) yr^{-1} and (0.009-0.17) Tg(N) yr^{-1} for SO_4^{2-} dry and wet deposition, respectively. High uncertainty is found in EA perturbation case, where the model divergence are mainly from SO_2 wet and dry deposition and SO_4^{2-} wet deposition. In terms of NO_y deposition (Fig. 5(b)), the differences among models range (0.003-0.07) Tg(N) yr^{-1} for NO_2 dry deposition, and (0.07-0.55) Tg(N) yr^{-1} and (0.03-0.75) Tg(N) yr^{-1} for NO_3^- dry and wet deposition, respectively. The EA perturbation case also has the largest inter-model variation, with high uncertainty in simulating both the NO_3^- wet and dry deposition. In terms of NH_x deposition (Fig. 5(c)), the differences among models range (0.04-0.09) Tg(N) yr^{-1} for NH_3 dry deposition, and (0.008-0.15) Tg(N) yr^{-1} and (0.002-0.11) Tg(N) yr^{-1} for NH_4^+ dry and wet deposition, respectively. Both EA and SA perturbation cases have relatively high uncertainties on NH_4^+ dry deposition. Overall, the inter-model variation is considerably high under emission perturbation in Asian regions, especially EA. On one hand, the EA perturbation case assumes the largest amount of emission reductions among all cases (Table S3). On the other hand, model evaluation (Tan et al., 2018) reported high model bias in simulating the deposition in this region, and suggest an incomplete knowledge from the combined picture provided by observations and models.

4 Conclusion

This study assesses the impact of hemispheric transport on S and N deposition for 6 regions: North America (NA), Europe (EU), South Asia (SA), East Asia (EA), Russia (RU) and Middle East (ME), by using multi-model ensemble results from 11 models of HTAP II, with simulations under base case and 20% emission perturbation scenario for each region.

We investigate the export of S and N emissions from source regions. Results show that about 27-58%, 26-46% and 12-23% of the emitted S, NO_x and NH_3 emissions are deposited outside of the source regions (ranges are for different source regions). The most significant exports of emissions are: (1) transport between EU and RU. 10-14% of EU's emission is transported to RU

and 7-12% of RU's emission is transport to EU. (2) transport between EA and RU. 5% of EA's emission is transported to RU and 4-5% of RU's emission is transported to EA. (3) transport from SA to EA (4-9%). Most regions export 5-10% more emission in winter than summer, which is highly influenced by chemistry, precipitation amount and frequency, atmospheric mixing and transport patterns.

We explore the impact of hemispheric transport on deposition in receptor regions. Overall, 20% emission reduction in source regions could affect 1-10% of deposition on foreign continental regions and 1-14% on foreign coastal regions and the open ocean. The most significant impacts are from NA to the North Atlantic Ocean (2-14%), and from EA to North Pacific Ocean (2-12%) and to western NA (4-6%). The amounts of deposition brought by hemispheric transport range from 10^4-10^5 kg(S or N) $month^{-1}$ per 0.1° longitude (meridional sum). The impact on deposition via short-distance transport between neighbouring regions (i.e. EU to RU) is generally found throughout the whole year and slightly stronger in winter, while the long-range transport (i.e. from EA to NA) mainly occurs in spring and fall.

We compare the impact from own region emission and foreign transport on local deposition. The deposition in NA, SA and EA is dominated (~80%) by their own region emission, while EU, ME and RU receive 40-60% of deposition from hemispheric transport. In particular, Russian deposition is even equally contributed by foreign inputs and own region emission, with high contributions from two neighbouring source regions: EA (~20%) and EU (~15%). For some regions, upmost half of the hemispheric transport from foreign regions is deposited over their coastal regions. Deposition in coastal regions or the near-coastal open ocean is found twice more sensitive to long-range transport than non-coastal regions. For some coastal regions such as west coast of NA and west coast of EU, the impact of hemispheric transport is identical or even larger than that of own region emission control.

This study highlights the impact of hemispheric transport on deposition in coastal regions and the open ocean, which hasn't been fully studied in the literature. We therefore suggest further research on this impact on the mitigation of coastal and oceanic ecosystem, with regards to the increasing air pollutants in hemispheric outflow. We also find significant impact of hemispheric transport on deposition in relatively low emission regions such as RU. The impact on their ecosystem and human health requires further research. Meanwhile, there is still a portion of foreign impact that hasn't been attributed in this study (aggregated as other regions "OTH" in Fig. 6). For

instance, at least 4 regions (NA, EU, SA and ME) have shown considerable impact (2-10%) on the S and N deposition in North Africa. But since North Africa is not included as a receptor/source region in the perturbation experiments, it is hard to quantify the impact of long-range transport on its deposition. Meanwhile, Southeast Asia is regarded as a big emission contributor in Asia. It is important to establish an S-R relationship with other Asian regions. We suggest the future HTAP simulations to include these regions in the perturbation experiments.

Data availability. The model data can be downloaded from AeroCom database (http://iek8wikis.iek.fz-juelich.de/HTAPWiki/FrontPage) upon request.

Competing interests. The author declare that they have no conflict of interest.

Acknowledgements. We thank all participating modeling groups in HTAP II for providing the simulation data. The National Center for Atmospheric Research (NCAR) is funded by the National Science Foundation. The CESM project is supported by the National Science Foundation and the Office of Science (BER) of the U.S. Department of Energy. Computing resources were provided by the Climate Simulation Laboratory at NCAR's Computational and Information Systems Laboratory (CISL), sponsored by the National Science Foundation and other agencies. We acknowledge the support by NASA HAQAST (grant no. NNX16AQ19G). We also acknowledge the support by the supercomputer system of the National Institute for Environmental Studies, Japan, and the Environment Research and Technology Development Fund (S-12-3) of the Ministry of the Environment, Japan, JSPS KAKENHI (grant no. 5H01728)

References

Arndt, R. L., and Carmichael, G. R.: Long-range transport and deposition of sulfur in Asia, Water Air and Soil Pollution, 85, 2283-2288, 10.1007/BF01186174,1995.

Auvray, M., and Bey, I.: Long-range transport to Europe: Seasonal variations and implications for the European ozone budget, J Geophys Res-Atmos, 110, 10.1029/2004JD005503, 2005.

Bergstrom, A. K., and Jansson, M.: Atmospheric nitrogen deposition has caused nitrogen enrichment and eutrophication of lakes in the northern hemisphere, Global Change Biol, 12, 635-643, 10.1111/j.1365-2486.2006.01129.x, 2006.

Berntsen, T. K., Karlsdottir, S., and Jaffe, D. A.: Influence of Asian emissions on the composition of air reaching the North Western United States, Geophys Res Lett, 26, 2171-2174, 10.1029/1999GL900477, 1999.

Bey, I., Jacob, D. J., Logan, J. A., and Yantosca, R. M.: Asian chemical outflow to the Pacific in spring: Origins, pathways, and budgets, J Geophys Res-Atmos, 106, 23097-23113, 10.1029/2001jd000806, 2001.

Bian, H. S., Chin, M., Hauglustaine, D. A., Schulz, M., Myhre, G., Bauer, S. E., Lund, M. T., Karydis, V. A., Kucsera, T. L., Pan, X. H., Pozzer, A., Skeie, R. B., Steenrod, S. D., Sudo, K., Tsigaridis, K., Tsimpidi, A. P., and Tsyro, S. G.: Investigation of global particulate nitrate from the AeroCom phase III experiment, Atmospheric Chemistry and Physics, 17, 12911-12940, 10.5194/acp-17-12911-2017, 2017.

Bleeker, A., Hicks, W. K., Dentener, E., Galloway, J., and Erisman, J. W.: N deposition as a threat to the World's protected areas under the Convention on Biological Diversity, Environ Pollut, 159, 2280-2288, 10.1016/j.envpol.2010.10.036, 2011.

Bobbink, R., Hicks, K., Galloway, J., Spranger, T., Alkemade, R., Ashmore, M., Bustamante, M., Cinderby, S., Davidson, E., Dentener, F., Emmett, B., Erisman, J. W., Fenn, M., Gilliam, F., Nordin, A., Pardo, L., and De Vries, W.: Global assessment of nitrogen deposition effects on terrestrial plant diversity: a synthesis, Ecol. Appl., 20, 30-59, 10.1890/08-1140.1, 2010.

Bouwman, A. F., Van Vuuren, D. P., Derwent, R. G., and Posch, M.: A global analysis of acidification and eutrophication of terrestrial ecosystems, Water Air and Soil Pollution, 141, 349-382, 10.1023/a:1021398008726, 2002.

Brown-Steiner, B., and Hess, P.: Asian influence on surface ozone in the United States: A comparison of chemistry, seasonality, and transport mechanisms, J Geophys Res-Atmos, 116, 10.1029/2011jd015846, 2011.

Chin, M., Diehl, T., Tan, Q., Prospero, J. M., Kahn, R. A., Remer, L. A., Yu, H., Sayer, A. M., Bian, H., Geogdzhayev, I. V., Holben, B. N., Howell, S. G., Huebert, B. J., Hsu, N. C., Kim, D., Kucsera, T. L., Levy, R. C., Mishchenko, M. I., Pan, X., Quinn, P. K., Schuster, G. L., Streets, D. G., Strode, S. A., Torres, O., and Zhao, X. P.: Multi-decadal aerosol variations from 1980 to 2009: a perspective from observations and a global model, Atmospheric Chemistry and Physics, 14, 3657-3690, 10.5194/acp-14-3657-2014, 2014.

Clark, C. M., and Tilman, D.: Loss of plant species after chronic low-level nitrogen deposition to prairie grasslands, Nature, 451, 712-715, 10.1038/nature06503, 2008.

Dentener, F., Drevet, J., Lamarque, J. F., Bey, I., Eickhout, B., Fiore, A. M., Hauglustaine, D., Horowitz, L. W., Krol, M., Kulshrestha, U. C., Lawrence, M., Galy-Lacaux, C., Rast, S., Shindell, D., Stevenson, D., Van Noije, T., Atherton, C., Bell, N., Bergman, D., Butler, T., Cofala, J., Collins, B., Doherty, R., Ellingsen, K., Galloway, J., Gauss, M., Montanaro, V., Muller, J. F., Pitari, G., Rodriguez, J., Sanderson, M., Solmon, F., Strahan, S., Schultz, M.,

553 Sudo, K., Szopa, S., and Wild, O.: Nitrogen and sulfur deposition on regional and global
554 scales: A multimodel evaluation, Global Biogeochem Cy, 20, 21, 10.1029/2005gb002672,
555 2006.
556 Deolal, S. P., Staehelin, J., Brunner, D., Cui, J. B., Steinbacher, M., Zellweger, C., Henne, S.,
557 and Vollmer, M. K.: Transport of PAN and NOy from different source regions to the Swiss
558 high alpine site Jungfraujoch, Atmospheric Environment, 64, 103-115,
559 10.1016/j.atmosenv.2012.08.021, 2013.
560 Derwent, R. G., Stevenson, D. S., Collins, W. J., and Johnson, C. E.: Intercontinental transport
561 and the origins of the ozone observed at surface sites in Europe, Atmospheric Environment,
562 38, 1891-1901, 10.1016/j.atmosenv.2004.01.008, 2004.
563 Doney, S. C., Mahowald, N., Lima, I., Feely, R. A., Mackenzie, F. T., Lamarque, J. F., and
564 Rasch, P. J.: Impact of anthropogenic atmospheric nitrogen and sulfur deposition on ocean
565 acidification and the inorganic carbon system, Proceedings of the National Academy of
566 Sciences of the United States of America, 104, 14580-14585, 10.1073/pnas.0702218104,
567 2007.
568 Duce, R. A., LaRoche, J., Altieri, K., Arrigo, K. R., Baker, A. R., Capone, D. G., Cornell, S.,
569 Dentener, F., Galloway, J., Ganeshram, R. S., Geider, R. J., Jickells, T., Kuypers, M. M.,
570 Langlois, R., Liss, P. S., Liu, S. M., Middelburg, J. J., Moore, C. M., Nickovic, S., Oschlies,
571 A., Pedersen, T., Prospero, J., Schlitzer, R., Seitzinger, S., Sorensen, L. L., Uematsu, M.,
572 Ulloa, O., Voss, M., Ward, B., and Zamora, L.: Impacts of atmospheric anthropogenic
573 nitrogen on the open ocean, Science, 320, 893-897, 10.1126/science.1150369, 2008.
574 Duncan, B. N., and Bey, I.: A modeling study of the export pathways of pollution from Europe:
575 Seasonal and interannual variations (1987-1997), J Geophys Res-Atmos, 109,
576 10.1029/2003JD004079, 2004.
577 Duncan, B. N., West, J. J., Yoshida, Y., Fiore, A. M., and Ziemke, J. R.: The influence of
578 European pollution on ozone in the Near East and northern Africa, Atmospheric Chemistry
579 and Physics, 8, 2267-2283, 10.5194/acp-8-2267-2008, 2008.
580 Fiore, A. M., Dentener, F. J., Wild, O., Cuvelier, C., Schultz, M. G., Hess, P., Textor, C., Schulz,
581 M., Doherty, R. M., Horowitz, L. W., MacKenzie, I. A., Sanderson, M. G., Shindell, D. T.,
582 Stevenson, D. S., Szopa, S., Van Dingenen, R., Zeng, G., Atherton, C., Bergmann, D., Bey,
583 I., Carmichael, G., Collins, W. J., Duncan, B. N., Faluvegi, G., Folberth, G., Gauss, M.,
584 Gong, S., Hauglustaine, D., Holloway, T., Isaksen, I. S. A., Jacob, D. J., Jonson, J. E.,
585 Kaminski, J. W., Keating, T. J., Lupu, A., Marmer, E., Montanaro, V., Park, R. J., Pitari, G.,
586 Pringle, K. J., Pyle, J. A., Schroeder, S., Vivanco, M. G., Wind, P., Wojcik, G., Wu, S., and
587 Zuber, A.: Multimodel estimates of intercontinental source-receptor relationships for ozone
588 pollution, Journal of Geophysical Research, 114, 10.1029/2008jd010816, 2009.
589 Fu, J. S., Dong, X. Y., Gao, Y., Wong, D. C., and Lam, Y. F.: Sensitivity and linearity analysis
590 of ozone in East Asia: The effects of domestic emission and intercontinental transport,
591 Journal of the Air & Waste Management Association, 62, 13,
592 10.1080/10962247.2012.699014, 2012.
593 Galloway, J. N., Townsend, A. R., Erisman, J. W., Bekunda, M., Cai, Z. C., Freney, J. R.,
594 Martinelli, L. A., Seitzinger, S. P., and Sutton, M. A.: Transformation of the nitrogen cycle:
595 Recent trends, questions, and potential solutions, Science, 320, 889-892,
596 10.1126/science.1136674, 2008.
597 Galmarini, S., Koffi, B., Solazzo, E., Keating, T., Hogrefe, C., Schulz, M., Benedictow, A.,
598 Griesfeller, J. J., Janssens-Maenhout, G., Carmichael, G., Fu, J., and Dentener, F.: Technical

note: Coordination and harmonization of the multi-scale, multi-model activities HTAP2, AQMEII3, and MICS-Asia3: simulations, emission inventories, boundary conditions, and model output formats, Atmos. Chem. Phys., 17, 1543-1555, 10.5194/acp-17-1543-2017, 2017.

Glotfelty, T., Zhang, Y., Karamchandani, P., and Streets, D. G.: Will the role of intercontinental transport change in a changing climate?, Atmospheric Chemistry and Physics, 14, 9379-9402, 10.5194/acp-14-9379-2014, 2014.

Guerova, G., Bey, I., Attie, J. L., Martin, R. V., Cui, J., and Sprenger, M.: Impact of transatlantic transport episodes on summertime ozone in Europe, Atmospheric Chemistry and Physics, 6, 2057-2072, 10.5194/acp-6-2057-2006, 2006.

Guo, J. H., Liu, X. J., Zhang, Y., Shen, J. L., Han, W. X., Zhang, W. F., Christie, P., Goulding, K. W. T., Vitousek, P. M., and Zhang, F. S.: Significant Acidification in Major Chinese Croplands, Science, 327, 1008-1010, 10.1126/science.1182570, 2010.

Holzer, M., Hall, T. M., and Stull, R. B.: Seasonality and weather-driven variability of transpacific transport, J Geophys Res-Atmos, 110, 10.1029/2005jd006261, 2005.

Hudman, R. C., Jacob, D. J., Cooper, O. R., Evans, M. J., Heald, C. L., Park, R. J., Fehsenfeld, F., Flocke, F., Holloway, J., Hubler, G., Kita, K., Koike, M., Kondo, Y., Neuman, A., Nowak, J., Oltmans, S., Parrish, D., Roberts, J. M., and Ryerson, T.: Ozone production in transpacific Asian pollution plumes and implications for ozone air quality in California, J Geophys Res-Atmos, 109, 10.1029/2004JD004974, 2004.

Jacob, D. J., Logan, J. A., and Murti, P. P.: Effect of rising Asian emissions on surface ozone in the United States, Geophys Res Lett, 26, 2175-2178, 10.1029/1999gl900450, 1999.

Jaffe, D., Price, H., Parrish, D., Goldstein, A., and Harris, J.: Increasing background ozone during spring on the west coast of North America, Geophys Res Lett, 30, 10.1029/2003gl017024, 2003.

James, C. N., and Houze, R. A.: Modification of precipitation by coastal orography in storms crossing northern California, Mon Weather Rev, 133, 3110-3131, 10.1175/MWR3019.1, 2005.

Janssens, I. A., Dieleman, W., Luyssaert, S., Subke, J. A., Reichstein, M., Ceulemans, R., Ciais, P., Dolman, A. J., Grace, J., Matteucci, G., Papale, D., Piao, S. L., Schulze, E. D., Tang, J., and Law, B. E.: Reduction of forest soil respiration in response to nitrogen deposition, Nature Geoscience, 3, 315-322, 10.1038/ngeo844, 2010.

Janssens-Maenhout, G., Crippa, M., Guizzardi, D., Dentener, F., Muntean, M., Pouliot, G., Keating, T., Zhang, Q., Kurokawa, J., Wankmuller, R., van der Gon, H. D., Kuenen, J. J. P., Klimont, Z., Frost, G., Darras, S., Koffi, B., and Li, M.: HTAP_v2.2: a mosaic of regional and global emission grid maps for 2008 and 2010 to study hemispheric transport of air pollution, Atmospheric Chemistry and Physics, 15, 11411-11432, 10.5194/acp-15-11411-2015, 2015.

Jickells, T.: The role of air-sea exchange in the marine nitrogen cycle, Biogeosciences, 3, 271-280, 10.5194/bg-3-271-2006, 2006.

Jickells, T. D., Buitenhuis, E., Altieri, K., Baker, A. R., Capone, D., Duce, R. A., Dentener, F., Fennel, K., Kanakidou, M., LaRoche, J., Lee, K., Liss, P., Middelburg, J. J., Moore, J. K., Okin, G., Oschlies, A., Sarin, M., Seitzinger, S., Sharples, J., Singh, A., Suntharalingam, P., Uematsu, M., and Zamora, L. M.: A reevaluation of the magnitude and impacts of anthropogenic atmospheric nitrogen inputs on the ocean, Global Biogeochem Cy, 31, 289-305, 10.1002/2016GB005586, 2017.

Kanakidou, M., Myriokefalitakis, S., Daskalakis, N., Fanourgakis, G., Nenes, A., Baker, A. R., Tsigaridis, K., and Mihalopoulos, N.: Past, Present, and Future Atmospheric Nitrogen Deposition, Journal of the Atmospheric Sciences, 73, 2039-2047, 10.1175/jas-d-15-0278.1, 2016.

Kim, T. W., Lee, K., Najjar, R. G., Jeong, H. D., and Jeong, H. J.: Increasing N Abundance in the Northwestern Pacific Ocean Due to Atmospheric Nitrogen Deposition, Science, 334, 505-509, 10.1126/science.1206583, 2011.

Lamarque, J. F., Kiehl, J. T., Brasseur, G. P., Butler, T., Cameron-Smith, P., Collins, W. D., Collins, W. J., Granier, C., Hauglustaine, D., Hess, P. G., Holland, E. A., Horowitz, L., Lawrence, M. G., McKenna, D., Merilees, P., Prather, M. J., Rasch, P. J., Rotman, D., Shindell, D., and Thornton, P.: Assessing future nitrogen deposition and carbon cycle feedback using a multimodel approach: Analysis of nitrogen deposition, J Geophys Res-Atmos, 110, 10.1029/2005jd005825, 2005.

Lamarque, J. F., Dentener, F., McConnell, J., Ro, C. U., Shaw, M., Vet, R., Bergmann, D., Cameron-Smith, P., Dalsoren, S., Doherty, R., Faluvegi, G., Ghan, S. J., Josse, B., Lee, Y. H., MacKenzie, I. A., Plummer, D., Shindell, D. T., Skeie, R. B., Stevenson, D. S., Strode, S., Zeng, G., Curran, M., Dahl-Jensen, D., Das, S., Fritzsche, D., and Nolan, M.: Multi-model mean nitrogen and sulfur deposition from the Atmospheric Chemistry and Climate Model Intercomparison Project (ACCMIP): evaluation of historical and projected future changes, Atmospheric Chemistry and Physics, 13, 7997-8018, 10.5194/acp-13-7997-2013, 2013.

Li, M., Liu, H., Geng, G. N., Hong, C. P., Liu, F., Song, Y., Tong, D., Zheng, B., Cui, H. Y., Man, H. Y., Zhang, Q., and He, K. B.: Anthropogenic emission inventories in China: a review, Natl Sci Rev, 4, 834-866, 10.1093/nsr/nwx150, 2017.

Li, Q. B., Jacob, D. J., Bey, I., Palmer, P. I., Duncan, B. N., Field, B. D., Martin, R. V., Fiore, A. M., Yantosca, R. M., Parrish, D. D., Simmonds, P. G., and Oltmans, S. J.: Transatlantic transport of pollution and its effects on surface ozone in Europe and North America, J Geophys Res-Atmos, 107, 10.1029/2001jd001422, 2002.

Li, Q. B., Jacob, D. J., Munger, J. W., Yantosca, R. M., and Parrish, D. D.: Export of NOy from the North American boundary layer: Reconciling aircraft observations and global model budgets, J Geophys Res-Atmos, 109, 10.1029/2003JD004086, 2004.

Li, X. Y., Liu, J. F., Mauzerall, D. L., Emmons, L. K., Walters, S., Horowitz, L. W., and Tao, S.: Effects of trans-Eurasian transport of air pollutants on surface ozone concentrations over Western China, J Geophys Res-Atmos, 119, 12338-12354, 10.1002/2014jd021936, 2014.

Liang, Q., Jaegle, L., Jaffe, D. A., Weiss-Penzias, P., Heckman, A., and Snow, J. A.: Long-range transport of Asian pollution to the northeast Pacific: Seasonal variations and transport pathways of carbon monoxide, J Geophys Res-Atmos, 109, 10.1029/2003JD004402, 2004.

Lin, M., Holloway, T., Carmichael, G. R., and Fiore, A. M.: Quantifying pollution inflow and outflow over East Asia in spring with regional and global models, Atmospheric Chemistry and Physics, 10, 4221-4239, 10.5194/acp-10-4221-2010, 2010.

Liu, H. Y., Jacob, D. J., Bey, I., Yantosca, R. M., Duncan, B. N., and Sachse, G. W.: Transport pathways for Asian pollution outflow over the Pacific: Interannual and seasonal variations, J Geophys Res-Atmos, 108, 10.1029/2002jd003102, 2003.

Liu, J. F., Mauzerall, D. L., and Horowitz, L. W.: Analysis of seasonal and interannual variability in transpacific transport, J Geophys Res-Atmos, 110, 10.1029/2004jd005207, 2005.

691 Liu, F., Zhang, Q., Ronald, J. V., Zheng, B., Tong, D., Yan, L., Zheng, Y. X., and He, K. B.:
692 Recent reduction in NOx emissions over China: synthesis of satellite observations and
693 emission inventories, Environ Res Lett, 11, 10.1088/1748-9326/11/11/114002, 2016.
694 Lu, Z., Streets, D. G., Zhang, Q., Wang, S., Carmichael, G. R., Cheng, Y. F., Wei, C., Chin, M.,
695 Diehl, T., and Tan, Q.: Sulfur dioxide emissions in China and sulfur trends in East Asia since
696 2000, Atmospheric Chemistry and Physics, 10, 6311-6331, 10.5194/acp-10-6311-2010,
697 2010.
698 Moxim, W. J., Levy, H., and Kasibhatla, P. S.: Simulated global tropospheric PAN: Its transport
699 and impact on NOx, J Geophys Res-Atmos, 101, 12621-12638, 10.1029/96jd00338, 1996.
700 Paerl, H. W.: Connecting atmospheric nitrogen deposition to coastal eutrophication,
701 Environmental science & technology, 36, 323a-326a, 10.1021/es022392a, 2002.
702 Parrish, D. D., Dunlea, E. J., Atlas, E. L., Schauffler, S., Donnelly, S., Stroud, V., Goldstein, A.
703 H., Millet, D. B., McKay, M., Jaffe, D. A., Price, H. U., Hess, P. G., Flocke, F., and Roberts,
704 J. M.: Changes in the photochemical environment of the temperate North Pacific troposphere
705 in response to increased Asian emissions, Journal of Geophysical Research: Atmospheres,
706 109, 10.1029/2004jd004978, 2004.
707 Parrish, D. D., Millet, D. B., and Goldstein, A. H.: Increasing ozone in marine boundary layer
708 inflow at the west coasts of North America and Europe, Atmospheric Chemistry and Physics,
709 9, 1303-1323, 10.5194/acp-9-1303-2009, 2009.
710 Paulot, F., Jacob, D. J., and Henze, D. K.: Sources and Processes Contributing to Nitrogen
711 Deposition: An Adjoint Model Analysis Applied to Biodiversity Hotspots Worldwide,
712 Environmental science & technology, 47, 3226-3233, 10.1021/es3027727, 2013.
713 Phoenix, G. K., Hicks, W. K., Cinderby, S., Kuylenstierna, J. C. I., Stock, W. D., Dentener, F. J.,
714 Giller, K. E., Austin, A. T., Lefroy, R. D. B., Gimeno, B. S., Ashmore, M. R., and Ineson, P.:
715 Atmospheric nitrogen deposition in world biodiversity hotspots: the need for a greater global
716 perspective in assessing N deposition impacts, Global Change Biol, 12, 470-476,
717 10.1111/j.1365-2486.2006.01104.x, 2006.
718 Reidmiller, D. R., Fiore, A. M., Jaffe, D. A., Bergmann, D., Cuvelier, C., Dentener, F. J.,
719 Duncan, B. N., Folberth, G., Gauss, M., Gong, S., Hess, P., Jonson, J. E., Keating, T., Lupu,
720 A., Marmer, E., Park, R., Schultz, M. G., Shindell, D. T., Szopa, S., Vivanco, M. G., Wild,
721 O., and Zuber, A.: The influence of foreign vs. North American emissions on surface ozone
722 in the US, Atmospheric Chemistry and Physics, 9, 5027-5042, 10.5194/acp-9-5027-2009,
723 2009.
724 Richter, A., Burrows, J. P., Nuss, H., Granier, C., and Niemeier, U.: Increase in tropospheric
725 nitrogen dioxide over China observed from space, Nature, 437, 129-132,
726 10.1038/nature04092, 2005.
727 Sanderson, M. G., Dentener, F. J., Fiore, A. M., Cuvelier, C., Keating, T. J., Zuber, A., Atherton,
728 C. S., Bergmann, D. J., Diehl, T., Doherty, R. M., Duncan, B. N., Hess, P., Horowitz, L. W.,
729 Jacob, D. J., Jonson, J. E., Kaminski, J. W., Lupu, A., MacKenzie, I. A., Mancini, E.,
730 Marmer, E., Park, R., Pitari, G., Prather, M. J., Pringle, K. J., Schroeder, S., Schultz, M. G.,
731 Shindell, D. T., Szopa, S., Wild, O., and Wind, P.: A multi-model study of the hemispheric
732 transport and deposition of oxidised nitrogen, Geophys Res Lett, 35, 10.1029/2008gl035389,
733 2008.
734 Stohl, A.: Characteristics of atmospheric transport into the Arctic troposphere, J Geophys Res-
735 Atmos, 111, 10.1029/2005JD006888, 2006.

Stohl, A., Trainer, M., Ryerson, T. B., Holloway, J. S., and Parrish, D. D.: Export of NOy from the North American boundary layer during 1996 and 1997 North Atlantic Regional Experiments, J Geophys Res-Atmos, 107, 10.1029/2001JD000519, 2002.

Sudo, K., and Akimoto, H.: Global source attribution of tropospheric ozone: Long-range transport from various source regions, J Geophys Res-Atmos, 112, 10.1029/2006JD007992, 2007.

Tan, J. N., Fu, J. S., Dentener, F., Sun, J., Emmons, L., Tilmes, S., Sudo, K., Flemming, J., Jonson, J. E., Gravel, S., Bian, H. S., Davila, Y., Henze, D. K., Lund, M. T., Kucsera, T., Takemura, T., and Keating, T.: Multi-model study of HTAP II on sulfur and nitrogen deposition, Atmospheric Chemistry and Physics, 18, 6847-6866, 10.5194/acp-18-6847-2018, 2018.

Tao, Z. N., Yu, H. B., and Chin, M.: Impact of transpacific aerosol on air quality over the United States: A perspective from aerosol-cloud-radiation interactions, Atmospheric Environment, 125, 48-60, 10.1016/j.atmosenv.2015.10.083, 2016.

van der A, R. J., Peters, D. H. M. U., Eskes, H., Boersma, K. F., Van Roozendael, M., De Smedt, I., and Kelder, H. M.: Detection of the trend and seasonal variation in tropospheric NO2over China, Journal of Geophysical Research, 111, 10.1029/2005jd006594, 2006.

van der A, R. J., Eskes, H. J., Boersma, K. F., van Noije, T. P. C., Van Roozendael, M., De Smedt, I., Peters, D. H. M. U., and Meijer, E. W.: Trends, seasonal variability and dominant NOxsource derived from a ten year record of NO2measured from space, Journal of Geophysical Research, 113, 10.1029/2007jd009021, 2008.

Verstraeten, W. W., Neu, J. L., Williams, J. E., Bowman, K. W., Worden, J. R., and Boersma, K. F.: Rapid increases in tropospheric ozone production and export from China, Nature Geoscience, 8, 690-+, 10.1038/ngeo2493, 2015.

Vet, R., Artz, R. S., Carou, S., Shaw, M., Ro, C. U., Aas, W., Baker, A., Bowersox, V. C., Dentener, F., Galy-Lacaux, C., Hou, A., Pienaar, J. J., Gillett, R., Forti, M. C., Gromov, S., Hara, H., Khodzher, T., Mahowald, N. M., Nickovic, S., Rao, P. S. P., and Reid, N. W.: A global assessment of precipitation chemistry and deposition of sulfur, nitrogen, sea salt, base cations, organic acids, acidity and pH, and phosphorus, Atmospheric Environment, 93, 3-100, 10.1016/j.atmosenv.2013.10.060, 2014.

Wild, O., and Akimoto, H.: Intercontinental transport of ozone and its precursors in a three-dimensional global CTM, J Geophys Res-Atmos, 106, 27729-27744, 10.1029/2000jd000123, 2001.

Wild, O., Pochanart, P., and Akimoto, H.: Trans-Eurasian transport of ozone and its precursors, J Geophys Res-Atmos, 109, 10.1029/2003jd004501, 2004.

WMO, 2017: Global Atmopshere Watch Workshop on Measurement-Model Fusion for Global Total Atmospheric Deposition (MMF-GTAD), GAW Report No. 234. Available at https://www.wmo.int/pages/prog/arep/gaw/documents/FINAL_GAW_234_23_May.pdf

Xavier, A., Kottayil, A., Mohanakumar, K., and Xavier, P. K.: The role of monsoon low-level jet in modulating heavy rainfall events, Int J Climatol, 38, E569-E576, 10.1002/joc.5390, 2018.

Yienger, J. J., Galanter, M., Holloway, T. A., Phadnis, M. J., Guttikunda, S. K., Carmichael, G. R., Moxim, W. J., and Levy, H.: The episodic nature of air pollution transport from Asia to North America, J Geophys Res-Atmos, 105, 26931-26945, 10.1029/2000jd900309, 2000.

Yu, H., M. Chin, L.A. Remer, H. Bian, Q. Tan, T. Yuan and Y. Zhang, Aerosols from overseas rival domestic emissions over North America, *Science*, Vol. 337, no. 6094, pp. 566-569, doi: 10.1126/science.1217576, 3 August. 2012.

Yu, H. B., Chin, M., West, J. J., Atherton, C. S., Bellouin, N., Bergmann, D., Bey, I., Bian, H. S., Diehl, T., Forberth, G., Hess, P., Schulz, M., Shindell, D., Takemura, T., and Tan, Q.: A multimodel assessment of the influence of regional anthropogenic emission reductions on aerosol direct radiative forcing and the role of intercontinental transport, J Geophys Res-Atmos, 118, 700-720, 10.1029/2012jd018148, 2013.

Zhang, L., Jacob, D. J., Boersma, K. F., Jaffe, D. A., Olson, J. R., Bowman, K. W., Worden, J. R., Thompson, A. M., Avery, M. A., Cohen, R. C., Dibb, J. E., Flock, F. M., Fuelberg, H. E., Huey, L. G., McMillan, W. W., Singh, H. B., and Weinheimer, A. J.: Transpacific transport of ozone pollution and the effect of recent Asian emission increases on air quality in North America: an integrated analysis using satellite, aircraft, ozonesonde, and surface observations, Atmospheric Chemistry and Physics, 8, 6117-6136, 10.5194/acp-8-6117-2008, 2008.

Zhang, L., Jacob, D. J., Kopacz, M., Henze, D. K., Singh, K., and Jaffe, D. A.: Intercontinental source attribution of ozone pollution at western US sites using an adjoint method, Geophys Res Lett, 36, 5, 10.1029/2009gl037950, 2009.

Zhang, L., Jacob, D. J., Knipping, E. M., Kumar, N., Munger, J. W., Carouge, C. C., van Donkelaar, A., Wang, Y. X., and Chen, D.: Nitrogen deposition to the United States: distribution, sources, and processes, Atmospheric Chemistry and Physics, 12, 4539-4554, 10.5194/acp-12-4539-2012, 2012.

Zhang, Q., Streets, D. G., He, K., Wang, Y., Richter, A., Burrows, J. P., Uno, I., Jang, C. J., Chen, D., Yao, Z., and Lei, Y.: NOx emission trends for China, 1995-2004: The view from the ground and the view from space, J Geophys Res-Atmos, 112, 10.1029/2007jd008684, 2007.

Figure captions:

Fig. 1. Administration boundaries of regions and coastal areas. 6 Regions with perturbation experiments: 3-North America (NA), 4-Europe (EU), 5-South Asia (SA), 6-East Asia (EA), 11-Middle East (MD) and 14-Russia, Belarussia, Ukraine (RU). Other regions: 1-Global, 2-Ocean (including Arctic), 7-Southeast Asia, 8-Australia, 9-North Africa, 10- Sub Saharan Africa, 12-Mexico, Central America, Caribbean, Guyanas, Venezuela, Columbia (Central America), 13-South America, 15-Central Asia and 17-Antarctic.

Fig. 2 The response of S deposition to 20% emission reduction in source regions. The values are the percentage changes (%) in deposition calculated as (changes in deposition with 20% emission reduction) / (base case deposition) ×100%. The unit is % per 0.1×0.1° grid box.

Fig.3 Same as Fig.2 but for NO_y deposition. The unit is % per 0.1×0.1° grid box.

Fig. 4 The monthly changes of S deposition with 20% emission reduction in source regions. The values are meridional total values versus time with a west-east resolution of 0.1 degree. The unit is $\times 10^4$ kg(S) $month^{-1}$ per 0.1º longitude. The negative values indicate decline in deposition with reduction in emission.

Fig. 5 Same as Fig.4 but for NO_y deposition. The unit is $\times 10^4$ kg(N) $month^{-1}$ per 0.1º longitude.

Fig. 6 Own region and foreign contributions on own region deposition. The values are calculated by changes with 20% emission reduction. Other (OTH, pattern fill) is the contribution by other reasons than emission reduction in the 6 regions (see text for details).

Fig. 7 Inter-model variations in deposition changes (unit: Tg(S or N) yr^{-1}) under emission perturbation experiments. The values are MMM with error bars showing the max and min values among all models.

Fig. 1

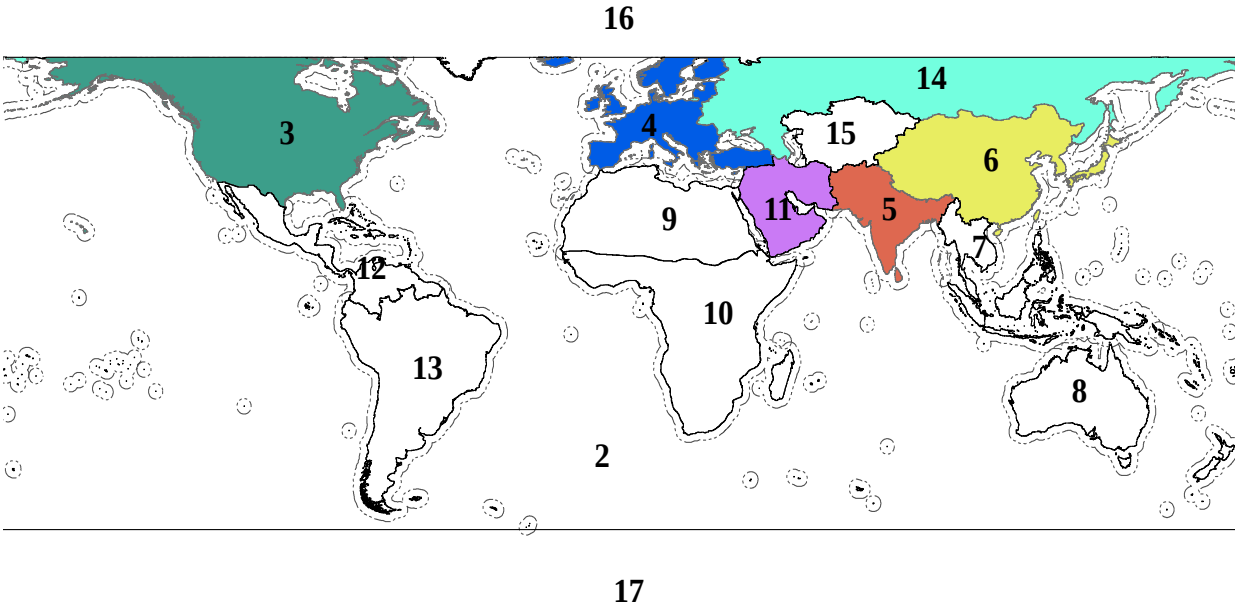

Fig. 1. Boundaries of regions and coastal areas (dashed). 6 Regions with perturbation experiments: 3-North America (NA), 4-Europe (EU), 5-South Asia (SA), 6-East Asia (EA), 11-Middle East (ME) and 14-Russia, Belarussia, Ukraine (RU). Others: 1-Global, 2-Ocean (including Arctic), 7-Southeast Asia, 8-Australia, 9-North Africa, 10- Sub Saharan Africa, 12- Mexico, Central America, Caribbean, Guyanas, Venezuela, Columbia (Central America), 13-South America, 15-Central Asia, 16-Arctic and 17-Antarctic.

Fig. 2

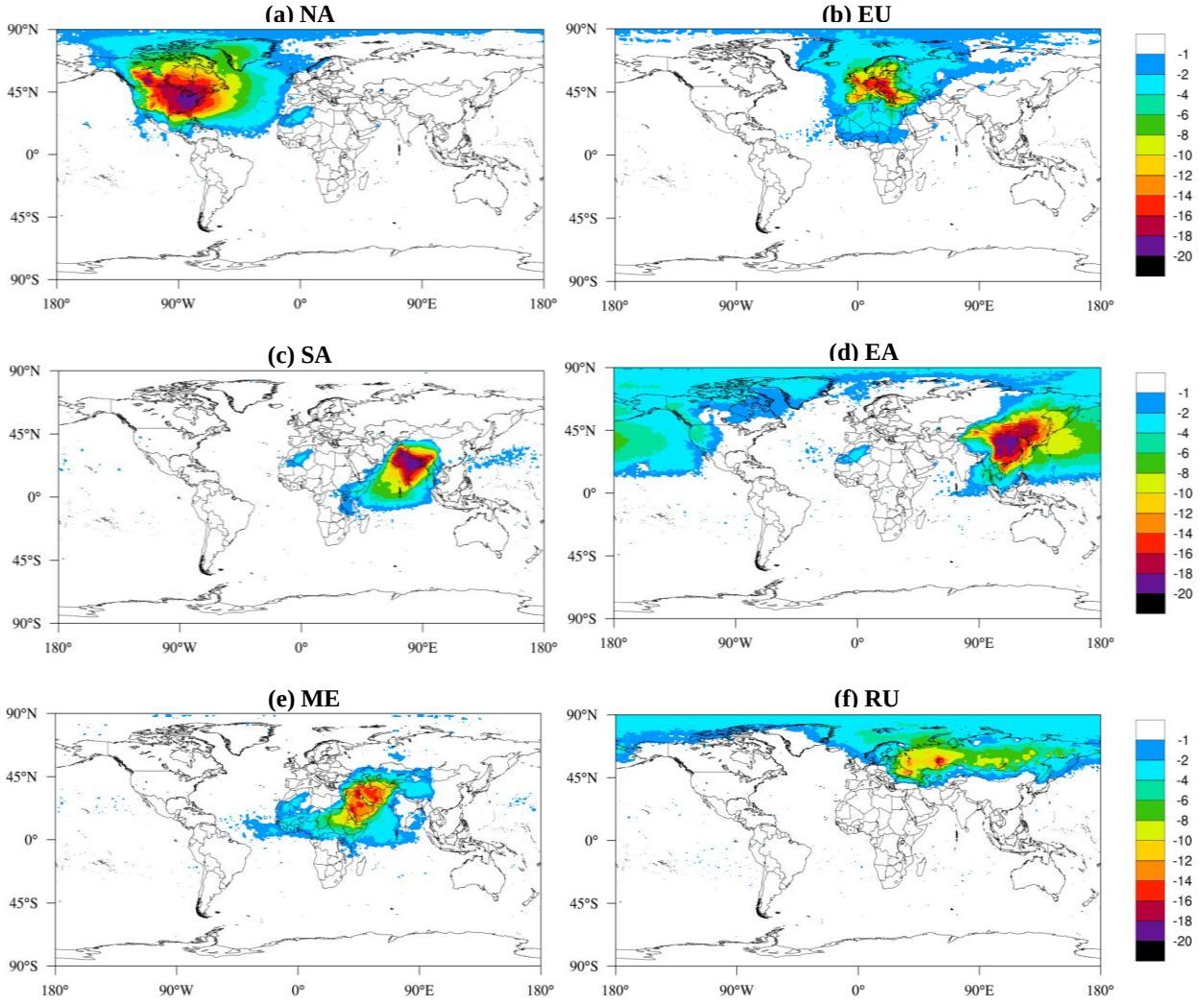

Fig. 2 The response of S deposition to 20% emission reduction in source regions. The values are the percentage changes (%) in deposition calculated as (changes in deposition with 20% emission reduction) / (base case deposition) ×100%. The unit is % per 0.1×0.1° grid box.

Fig. 3

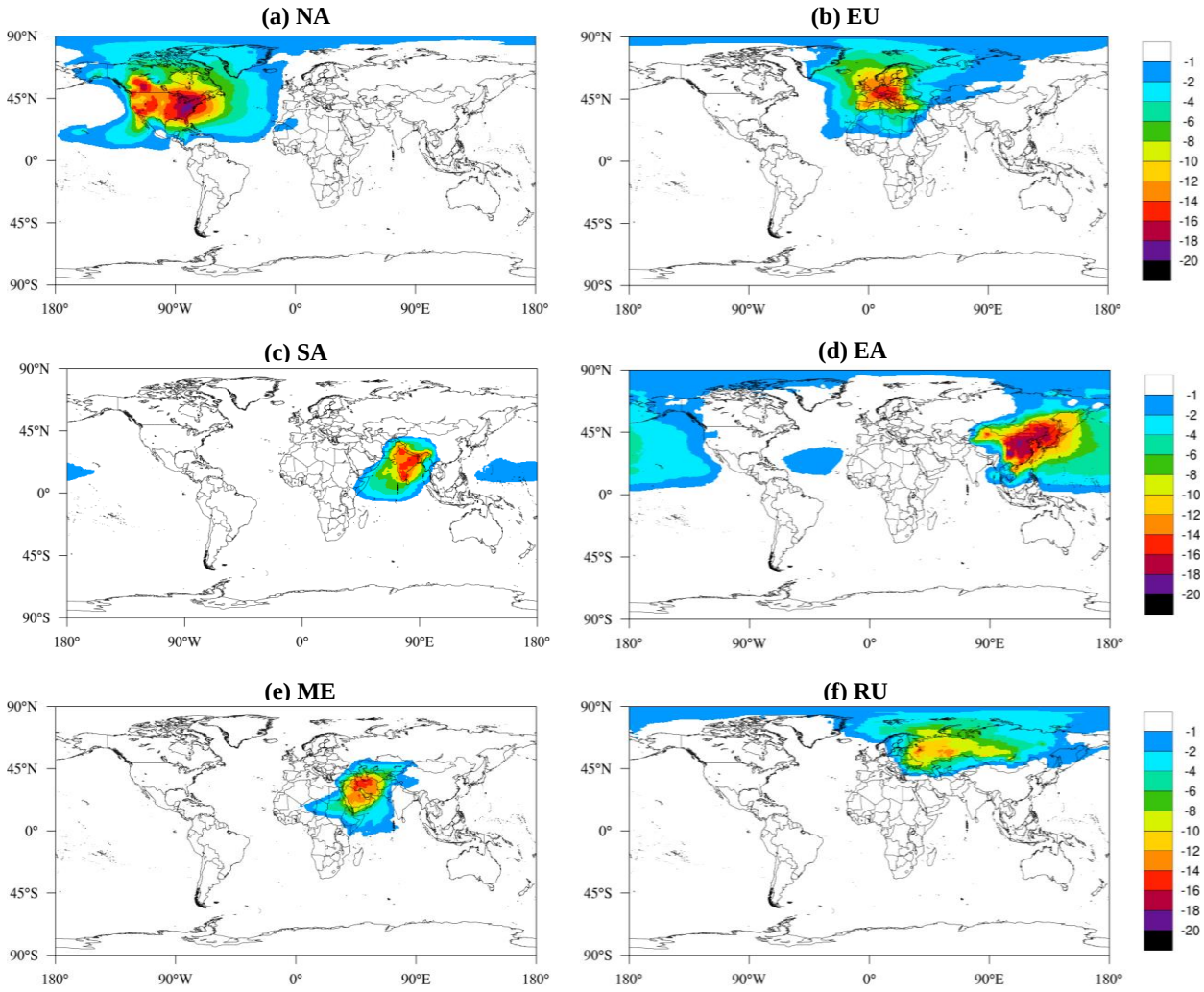

Fig.3 Same as Fig.2 but for NO_y deposition. The unit is % per 0.1×0.1° grid box.

Fig. 4

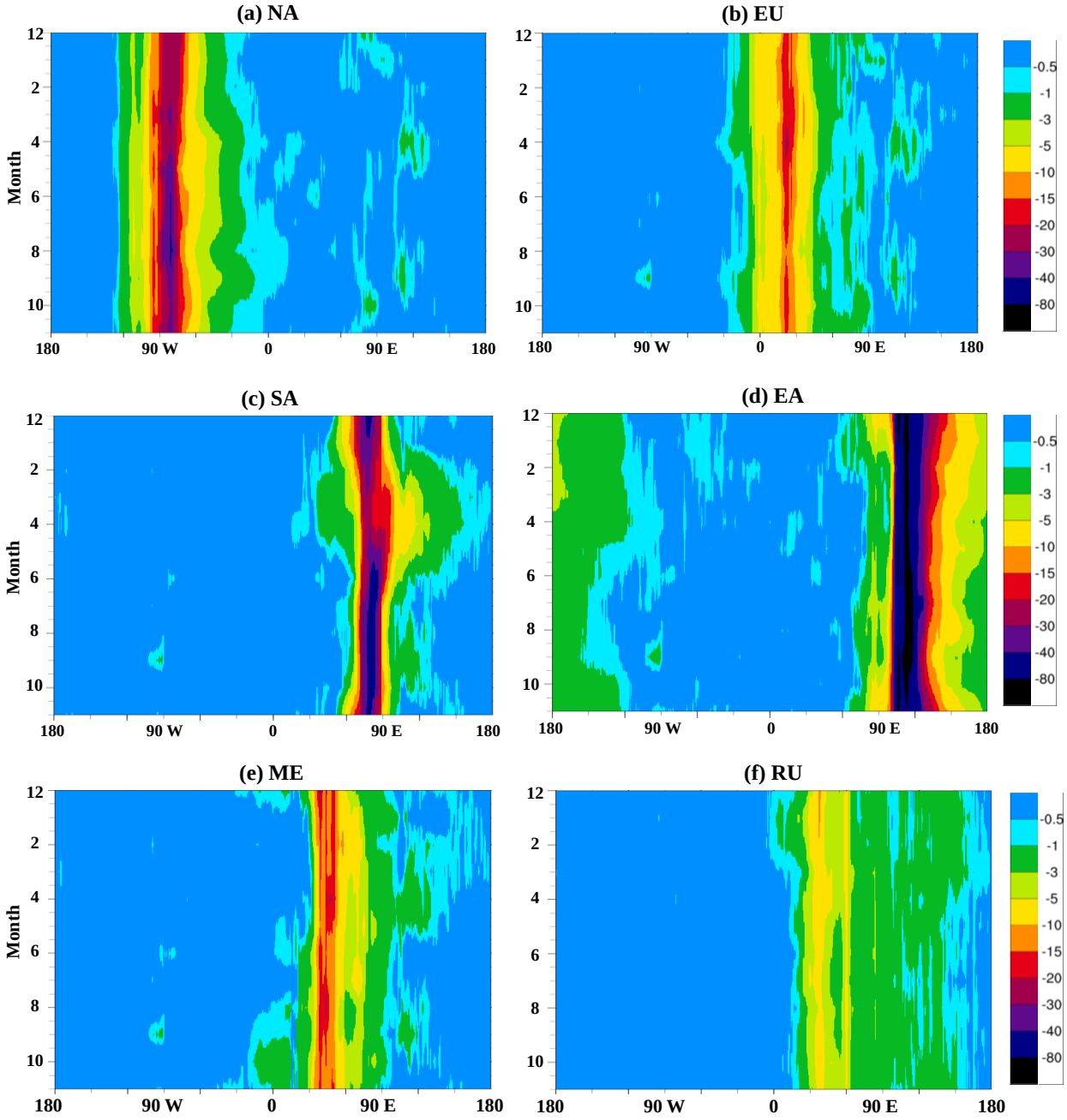

Fig. 4 The monthly changes of S deposition with 20% emission reduction in source regions. The x-axis values are meridional total values versus time (y-axis) with a west-east resolution of 0.1 degree. The unit is $\times 10^4$ kg(S) $month^{-1}$ per 0.1° longitude. Negative values indicate decline in deposition with reduction in emission.

Fig. 5

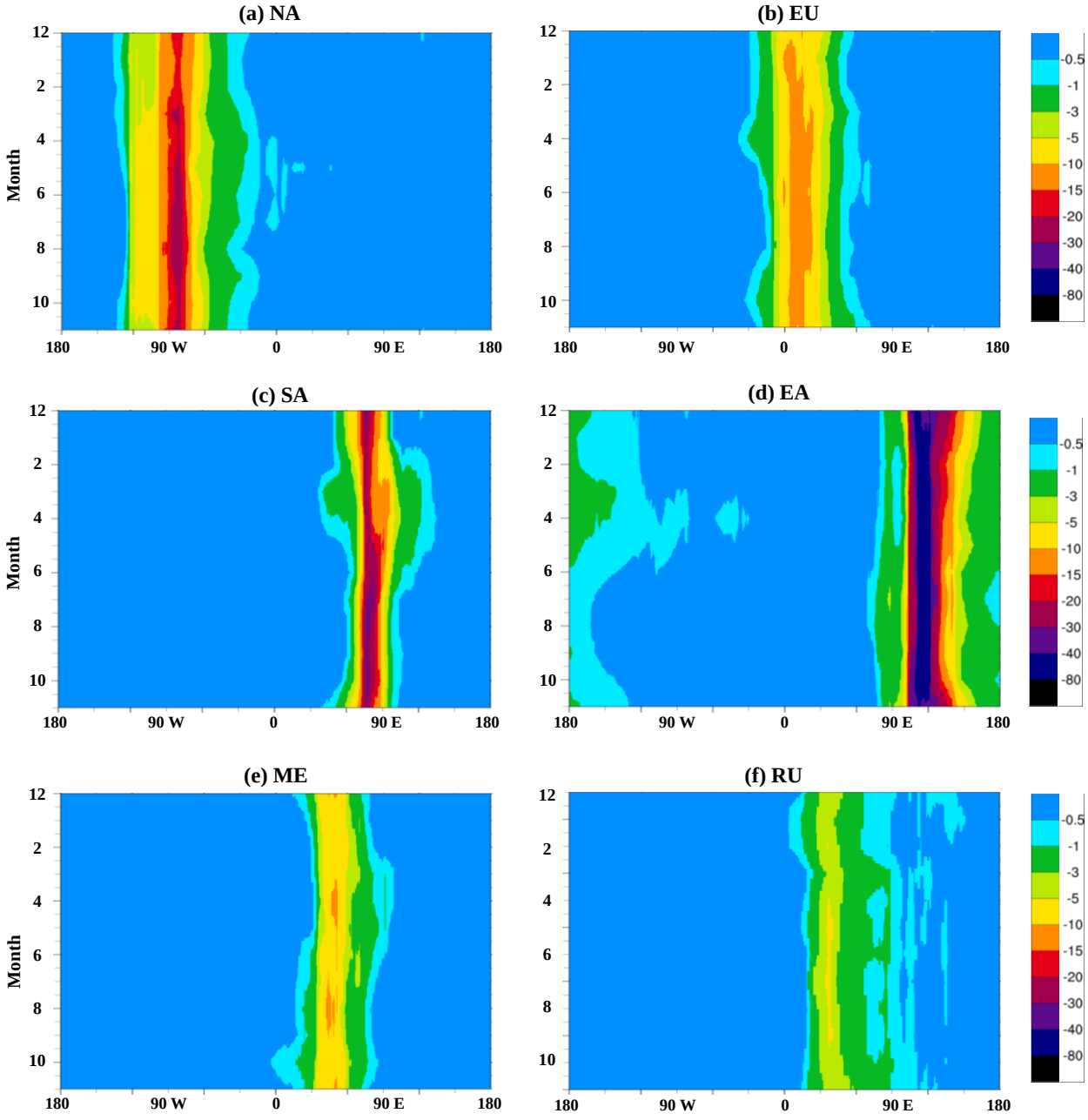

Fig. 5 Same as Fig.4 but for NO_y deposition. The unit is $\times 10^4$ kg(N) $month^{-1}$ per 0.1° longitude.

Fig. 6

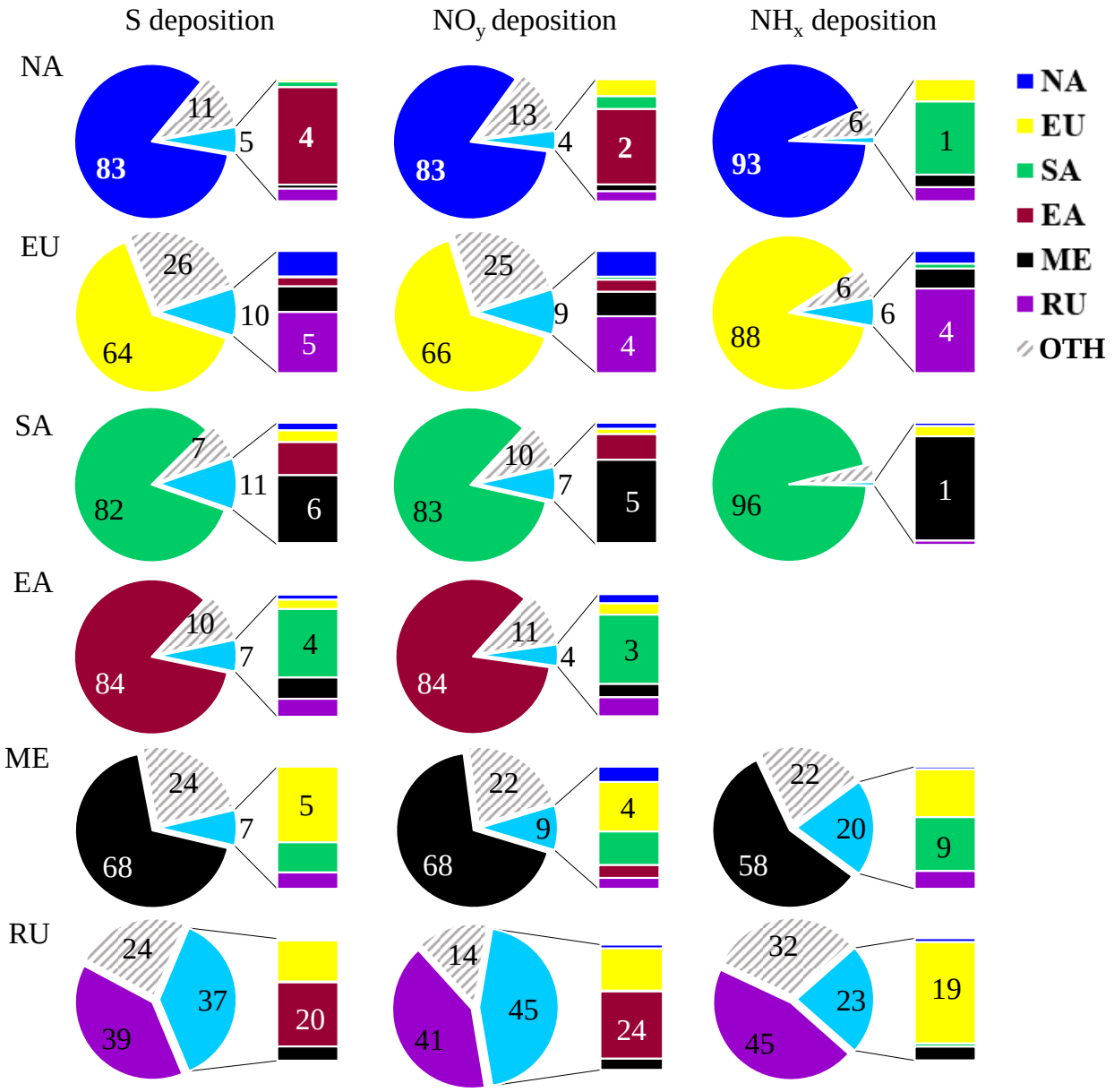

Fig. 6 Own region and foreign contributions on own region deposition. The values are calculated by changes with 20% emission reduction. Other (OTH, pattern fill) is the contribution by other reasons than emission reduction in the 6 regions (see text for details).

868 **Fig. 7**

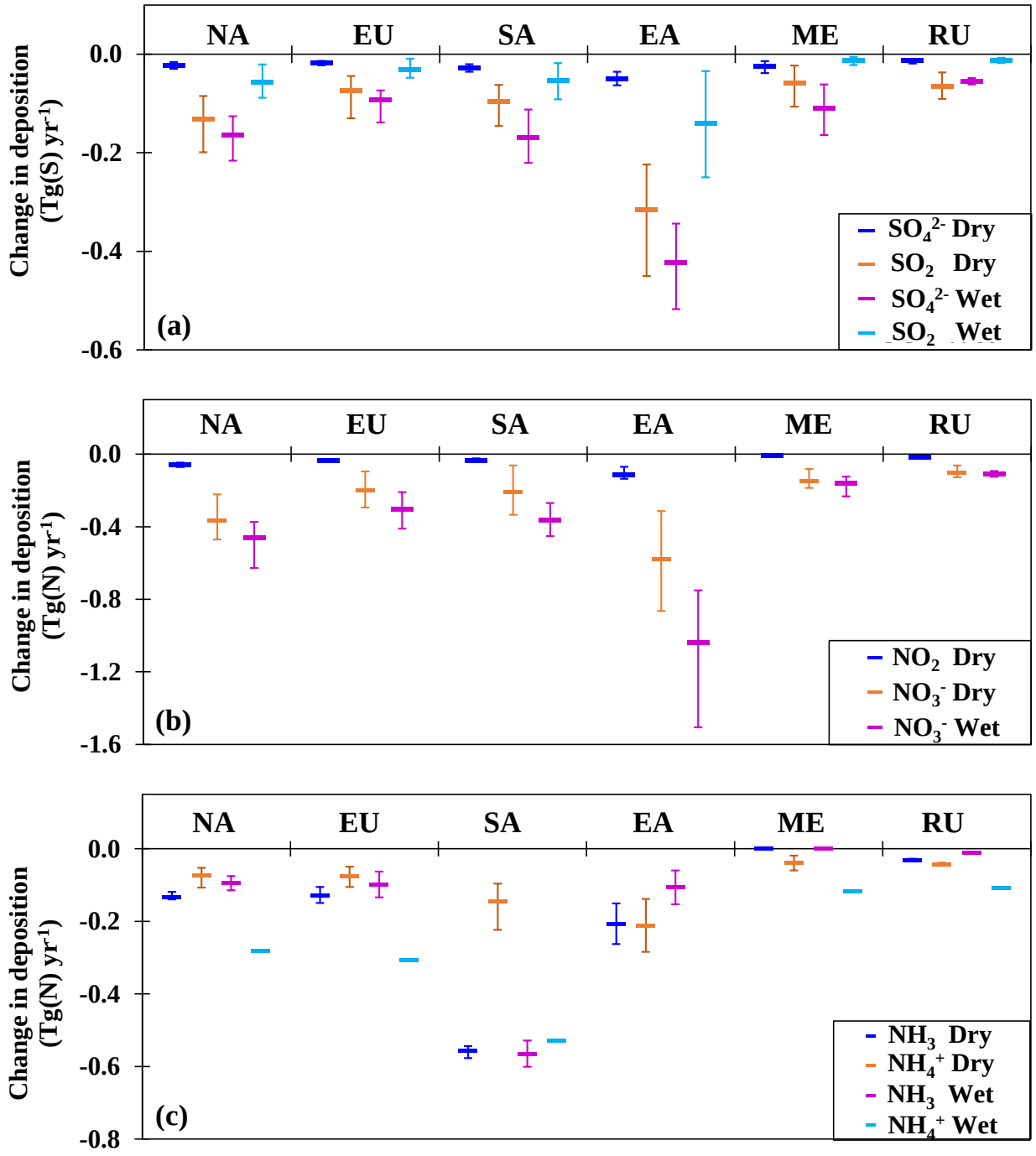

869
870 Fig. 7 Inter-model variations in wet and dry deposition changes (unit: Tg(S or N) yr^{-1}) under
871 emission perturbation experiments. The values are global integrated changes in components of S
872 and N deposition for perturbation experiments from MMM results with error bars showing the
873 max and min values among all models. Species without error bars are derived from results of a
874 single model.

875

Tables

Table 1. Source-receptor relationship of $S/NO_y/NH_x$ deposition (%) for regions (including continental coastal and non-coastal regions). The values in the parentheses are for coastal regions as a subset of the total.

	Receptor Regions	Source Regions					
		NA	EU	SA	EA	ME	RU
S Deposition	NA	68.9 (8.9)	0.2 (0.1)	0.2 (0.0)	1.5 (0.6)	0.3 (0.1)	1.2 (0.6)
	EU	1.1 (0.6)	60.4 (14.4)	0.0 (0.0)	0.2 (0.1)	2.1 (0.2)	6.9 (2.5)
	SA	0.5 (0.1)	1.2 (0.3)	66.4 (10.0)	0.9 (0.4)	7.9 (1.6)	0.3 (0.1)
	EA	0.6 (0.2)	1.8 (0.4)	8.8 (1.3)	73.4 (11.5)	4.6 (0.8)	5.2 (1.4)
	ME	0.0 (0.0)	2.6 (0.6)	0.6 (0.3)	0.0 (0.0)	42.4 (8.2)	0.8 (0.2)
	RU	0.4 (0.1)	13.6 (2.2)	0.1 (0.1)	5.1 (2.2)	5.0 (1.1)	62.2 (4.4)
	Others	28.5	20.1	23.8	19.1	37.7	23.4
NO_y Deposition	NA	71.5 (7.8)	0.8 (0.2)	0.5 (0.1)	1.0 (0.3)	0.5 (0.1)	1.0 (0.3)
	EU	1.3 (0.6)	66.2 (17.5)	0.2 (0.1)	0.3 (0.1)	3.5 (0.9)	9.8 (2.9)
	SA	0.2 (0.0)	0.2 (0.0)	66.2 (8.6)	0.5 (0.2)	7.9 (1.3)	0.2 (0.0)
	EA	0.6 (0.1)	1.2 (0.2)	6.2 (0.7)	74.4 (14.3)	2.4 (0.3)	4.3 (0.9)
	ME	0.4 (0.1)	1.6 (0.3)	0.9 (0.4)	0.1 (0.0)	54.4 (8.0)	0.8 (0.2)
	RU	0.6 (0.1)	10.3 (1.3)	0.1 (0.0)	5.1 (2.2)	4.9 (1.3)	61.4 (3.1)
	Others	25.6	19.7	25.8	18.6	26.4	22.5
NH_x Deposition	NA	88.4 (5.6)	0.2 (0.1)	0.3 (0.1)	-*	0.7 (0.3)	0.4 (0.2)
	EU	0.6 (0.3)	83.2 (17.8)	0.0 (0.0)	-	4.6 (1.2)	11.9 (3.1)
	SA	0.0 (0.0)	0.1 (0.0)	85.1 (7.6)	-	8.6 (2.4)	0.0 (0.0)
	EA	0.0 (0.0)	0.4 (0.1)	4.2 (0.3)	-	2.6 (0.5)	3.8 (1.0)
	ME	0.1 (0.0)	1.3 (0.3)	0.4 (0.2)	-	49.4 (5.9)	1.5 (0.4)
	RU	0.4 (0.1)	10.3 (1.3)	0.1 (0.0)	-	7.3 (1.5)	76.9 (4.1)
	Others	10.5	4.4	9.7	-	26.9	5.7

* Lack of NH_4^+ wet deposition under EA emission perturbation experiment from all models.

Table 2. Extra-regional emission reduction (RERER) values of S/NO_y/NH_x deposition for continent non-coastal and coastal regions. The RERER values are calculated by dividing the Δ Depo due to foreign emission reduction by Δ Depo due to global (foreign + own region) emission control. Total column gives the RERER for coastal and non-coastal together.

Regions	S deposition			NO_y deposition			NH_x deposition		
	Total	Non-coastal	Coastal	Total	Non-coastal	Coastal	Total	Non-coastal	Coastal
NA	0.17	0.12	0.40	0.17	0.12	0.43	0.07	0.05	0.31
EU	0.36	0.27	0.53	0.34	0.27	0.48	0.12	0.09	0.22
SA	0.18	0.14	0.35	0.17	0.12	0.37	0.04	0.03	0.17
EA	0.16	0.14	0.28	0.16	0.12	0.27	-	-	-
ME	0.32	0.27	0.46	0.32	0.27	0.50	0.42	0.36	0.67
RU	0.61	0.56	0.84	0.59	0.52	0.90	0.55	0.49	0.85